Arch. Metall. Mater., Vol. 61 (2016), No 4, p. 1825–1832

DOI: 10.1515/amm-2016-0295

A. RYBAK*#, AU. RYBAK**, W. KASZUWARA***

CHARACTERIZATION OF SELECTED PARAMETERS OF ORGANIC-INORGANIC HYBRID MEMBRANES BASED ON VARIOUS POLYMERS AND Nd-Fe-B FILLERS

In this paper magnetic organic-inorganic hybrid membranes based on EC, PPO polymer matrices and various magnetic powder microparticles were synthesized and studied. Constant pressure permeation technique and the Time Lag method were used to obtain the gas transport coefficients. The mechanical, rheological and magnetic parameters of magnetic hybrid membranes were examined. It was found that their separation and gas transport properties (*D, P, S* and α) were improved with the decrease in powder particle size and the increase of membrane's remanence, saturation magnetization and magnetic particle filling. The increase of the magnetic powder addition and a decrease of its granulation improved also mechanical and rheological parameters of the tested membranes. This improvement also had a positive effect on their gas separation properties and their potential usage in the future.

Keywords: organic-inorganic hybrid membranes, magnetic measurements, rheological parameters, mechanical properties, gas separation

1. Introduction

Nowadays, the development of membrane separation technologies allows their wider application in chemical and petrochemical industries. Commonly used polymeric and inorganic membranes have both advantages and disadvantages. Polymer membranes present usually high permeabilities to gases or vapours, and can produce thin films, but unfortunately they have lower thermal and chemical stability. While inorganic membranes exhibit usually high mechanical, thermal and chemical stability. However, they suffer from low processibility and higher costs than organic polymeric membranes. Thus, the main goal of the membrane technology development is the introduction of high-performance new materials [1, 2]. Recently, the studies of organic-inorganic hybrid materials (also known as mixed matrix membranes, MMMs) have attracted much attention. They have shown to be a promising new generation of membrane materials for the various potential applications such as gas separation (He, H_2, O_2, N2, CH_4, CO_2), pervaporation, membrane fuel cells (MFC) and direct methanol fuel cell (DMFC) applications. These materials combine the advantages of the two types of materials for separation purposes. That is the high processibility of polymers and the high selectivity and permeability of inorganic materials. That's why, various combinations of polymers and inorganic materials have been extensively studied in the last years. The most commonly used inorganic fillers are zeolites, carbon molecular sieves, silica, metal particles, carbon black, carbon fiber and metal oxides. Numerous hybrid systems based on various polymer matrices were used, such as: poly(caprolactone), poly(amide), polyimide, poly(styrene-co-methacrylate), polydimethylsiloxane (PDMS), polymethylpentene (PMP), polyaniline (PANI), polymethyl methacrylate (PMMA), polyvinyl alcohol (PVA) and many others [3-8]. They are materials of great interest for researchers because their properties, and the effectiveness of membrane activity can be adjusted by controlling the composition, content and morphology of the particle addition, by usage of different processing techniques and modification of the polymer matrix (improvement of the interaction between these two materials, their compatibility and dispersion of inorganic phase) [9]. Material and type of filler as well as it's amount in the composite have a significant influence on the physical and mechanical properties (thermal stability, optical, mechanical and gas separation properties) [10, 11]. Although, the production of these hybrid membranes is increasingly described in the literature, the scientists still are looking for solutions to improve their processibility, flux, selective gas separation and membrane durability. The reduction of potential problems could be also achieved using many methods, like chemical modification of the inorganic components surface using desired silanes and polymers or introduction of various compatibilizers [12-16]. Some effort has been also focused on producing organic–inorganic hybrid membranes containing magnetic fillers. There have been used many hybrid organic-inorganic systems with enhanced electrical and magnetic properties, like, for instance: non-conducting and conducting polymers PANI with Fe_3O_4, g-Fe_2O_3, NiZn ferrite, $BaFe_{12}O_{19}$,

* SILESIAN UNIVERSITY OF TECHNOLOGY, DEPARTMENT OF PHYSICAL CHEMISTRY AND TECHNOLOGY OF POLYMERS, FACULTY OF CHEMISTRY, 9 STRZODY STR., 44-100 GLIWICE, POLAND

** SILESIAN UNIVERSITY OF TECHNOLOGY, FACULTY OF MINING AND GEOLOGY, 2A AKADEMICKA STR., 44-100 GLIWICE, POLAND

*** WARSAW UNIVERSITY OF TECHNOLOGY , FACULTY OF MATERIALS SCIENCE AND ENGINEERING, 141,WOLOSKA STR., 02-507 WARSZAWA, POLAND

Corresponding author: aleksandra.rybak@polsl.pl

$MnFe_2O_4$ and SiO_2/Nd–Fe–B magnet, Fe_3O_4/rubber, $NiFe_2O_4$/polystyrene and hexaferrite/polymer [17-21]. It was also conducted research on magnetic core–shell nanocomposites using $Zn_{0.5}Co_{0.5}Al_{0.5}Fe_{1.46}La_{0.04}O_4$ as a core being surfactant with four different polymeric shells (PVP, PVA, PVAc and PEG) [25]. In recent years, our research has focused on magnetic hybrid organic-inorganic membranes used for the air enrichment in oxygen. We have used the potential difference between magnetic properties of paramagnetic oxygen and diamagnetic nitrogen, what has provided the differentiated conditions (other than sorption–diffusion) in mass transport of the separated gases and given the opportunity for their separation [26-32]. This paper is the continuation of our earlier works [28-34], which stated that the incorporation of magnetic micropowders into the polymer matrix (EC, PPO) improved the gas transport properties of produced membranes. In this work, we are going further to exam, the mechanical, rheological and magnetic properties of various magnetic hybrid membranes (EC and PPO with dispersed magnetic powders, like commercial MQP-14-12, MQP-16-7 and MQP-B with a particle size 5, 25 μm and 20-50 μm).

2. Experimental

2.1. Materials

Poly(2,6-dimethyl-1,4-phenylene oxide) (PPO) was supplied by Sabic Innovative Plastics, while the ethylcellulose (EC) by Acros Organics. The magnetic powders MQP-14-12, MQP-16-7 and MQP-B were used as an inorganic additive. The MQP-14-12 with a particle size 20-50 μm (D50=38 μm) were obtained during the milling of powder MQP-14-12 supplied by Magnequench. While the magnetic powders MQFP-14-12 with 5 and 25μm granulation (D50=5 μm and D50=25μm), MQFP-16-7 and MQFP-B with 5 μm granulation (with AA4 coating; D50=5 μm) are the products of Magnequench company. They are the isotropic magnetic powders, based on a patented Nd-Nb-Fe-B, Nd-Pr-Fe-B and Nd-Fe-Co-B alloy compositions. Ethanol, toluene and trichloroethylene (TCE) with 99% purities were supplied by Sigma Aldrich and Acros (Poland). Compressed cylinders of oxygen (5.6), nitrogen (5.0), helium (6.0) and synthetic air (5.0) were supplied by Linde Gas (Poland).

2.2. Description of membrane production process and experimental setup

In our studies, we have examined the hybrid organic-inorganic magnetic membranes of thickness 118-206 μm (depended on the amount and granulation of added magnetic powder). These membranes were cast from appropriate polymer (EC or PPO) solutions with the dispersed magnetic powders after sonication (of the appropriate amount: 1.0 – 1.75g and various granulations) in the external field of a coil (stable magnetic field 40 mT). Membranes were removed from Petri dish (with some distilled water) and dried in 40°C for at least two days before analysis. With this procedure, a series of membranes with an inorganic content ranging from 54.0 to 72.0 wt % was prepared. The permeation measurements were performed, before and after magnetization in an impulse inducteur, generating magnetic field induction approximately of 2.9 T. Nitrogen, oxygen and synthetic air permeability was measured by means of low-pressure gas permeation analyzer APG-1, described in the papers [26, 27, 32, 33]. The analysed membranes in the form of discs (membrane effective area 19.63 cm^2) were put in a diffusive chamber and rinsed with an analysed gas. Oxygen, nitrogen and synthetic air (21% O_2 and 79% N_2) were introduced to the setup from compressed gas cylinders. Then, we have established (0.3 – 0.9 MPa) and controlled the suitable pressure difference (electronic pressure meter and controller EL-press P-506C) between high- and low-pressure part of a chamber. After that, we have obtained the flow rate of permeate using Flow-Bus flowmeter (with a range 0-3 ml/min) with a computer data acquisition. All measurements were carried out in room temperature. The oxygen and nitrogen concentration in permeate was analysed using a gas chromatograph HP 5890A.

2.3. The evaluation of gas transport coefficients

We have collected experimental permeation data for the oxygen and nitrogen, both for individual, pure gases, as well as components of air. For their analysis was used Time Lag method [26]. Few important diffusion, permeability, solubility and selectivity coefficients, like: D_L, $\overline{D}$, P, S, α were obtained using this method [32, 33].

We have measured the flow rate Q (using a flowmeter) and then after conversion to standard conditions and dividing by the effective area of the membrane, we received diffusive mass flux in a stationary state J_S. From this mass flux we have assigned the mass transport coefficients based on the following formulas:

$$\overline{D} = \frac{J_s \cdot l}{\Delta c} \tag{1}$$

where:

$\overline{D}$- average diffusion coefficient [cm^2/s], J_s - diffusive mass flux in stationary state [$cm^3_{STP}/cm^2.s$],

l - thickness of membrane [cm], Δc- concentration difference [cm^3_{STP}/cm^3].

$$P = \frac{J_S\, l}{\Delta p} \tag{2}$$

where:

P – permeation coefficient [Barrer], $\frac{cm^3_{STP} \cdot cm}{cm^2 \cdot s \cdot cmHg} \cdot 10^{-10}$,

l – membrane thickness [cm],

Δ_p – gas pressure difference at both sides of the membrane [cmHg], J_s – diffusive mass flux in a stationary state $\left[\frac{cm^3_{STP}}{cm^2 \cdot}\right]$.

$$S - \frac{P}{\overline{D}} \tag{3}$$

where:

S - solubility coefficient $\left[\frac{cm^3_{STP}}{cm^3 \cdot cmHg}\right]$.

and

$$\alpha_{O2/N2} = \frac{P_{O2}}{P_{N2}} \quad (4)$$

where:
$\alpha_{O2/N2}$ - ideal selectivity coefficient, P_{O2}, P_{N2} – permeation coefficient of pure components [Barrer].

Precise description of the Time Lag method can be found in our previous papers [26, 27, 29, 35, 36]. After integration of J_S with respect to time, we have got a downstream absorption permeation $Q^a\ (l,\ t)$ (total flow of penetrant). According to this method the concentration difference Δc and Time Lag L^a were determined. The first one was obtained from an intercept of the asymptote to the stationary permeation curve with the $Q^a\ (l,\ t)$ axis. While the second one L^a was determined as an intercept of the asymptote to the stationary permeation curve with the time axis.

The next diffusion coefficient D_L was calculated from the downstream absorption Time Lag L^a [26, 27, 29] according to the following equation:

$$D_L = \frac{l^2}{6L^a(l)} \quad (5)$$

Comparing $\overline{D}$ with the value of diffusion coefficient D_L, we can get some insight into the nature of the transport process. If $\overline{D} = D_L$, the diffusion is supposed to be an "ideal Fickian" unless there are some other processes, like a drift [26, 29]. In this case, the drift coefficient w measures the strength of magnetic field that causes a preferred motion direction of the examined gas molecules (especially paramagnetic oxygen) through the membrane with respect to the field. To obtain the drift coefficient w_{Bi}, we have separated the drift and diffusion in an overall flux (assuming that diffusional contribution to the overall flux is magnetic field independent) and calculated from equation [26, 29]:

$$w_{Bi} = \frac{J_{Bi} - J_0}{\Delta c_0} \quad (6)$$

where:
w_{Bi} – drift coefficient [cm/s], J_{Bi} – oxygen flux for magnetic membrane with appropriate magnetic induction $B_i \left[\frac{\mathrm{cm}^3_{\mathrm{STP}}}{\mathrm{cm}^2 \cdot \mathrm{s}}\right]$, J_0 - oxygen flux for pure polymer membrane $\left[\frac{\mathrm{cm}^3_{\mathrm{STP}}}{\mathrm{cm}^2 \cdot \mathrm{s}}\right]$, Δc_0 - equilibrium concentration of oxygen [cm^3_{STP}/cm^3], B_i - magnetic induction of a membrane [T]. The obtained values of drift coefficient w_{Bi} are given in Table 3.

2.4. Characterization of hybrid membrane's magnetic properties

The magnetic properties of hybrid membranes were examined by means of a Lake Shore 7010 vibrating sample magnetometer (VSM). The samples cut from the membranes were placed in the magnetometer perpendicularly to the direction of the magnetic field (their thickness was negligibly small compared to their other dimensions). The measurements were made with the maximum intensity of the magnetic field: 2280 kA/m. Coercivity, saturation magnetization and remanence were determined based on the obtained magnetic hysteresis loops.

2.5. Mechanical and rheological properties of hybrid magnetic membranes

The microstructure of magnetic membrane's surfaces was observed by optic microscopy (microscope Nikon Epiphot 200 with a computer image analyzer), from which images are shown in Fig.3. The obtained magnetic hybrid membranes were also analysed using the X-ray micro-tomography (X-ray micro-tomograph SkyScan 1174), from which image is shown in Fig.4.

Hybrid membranes were examined with the use of static testing machine Zwick/Roell Z050 working in the range 50 kN force, with mechanical wedge holders to the flat samples. Tests were conducted in the room temperature with speed 0,5 mm/min. Rheological measurements were carried out using ARES rheometer from TA Instruments. In the rotary rheometer, due to the rotation of the measuring system element comes to sample shearing between the two surfaces. One plate is stationary while the other performs a rotational movement. The measurements were performed in dynamic mode in the plate-plate system at a constant value of strain amplitude γ =0.5% and variable angular frequency in the range of ω =0.1–79.4 Hz. Experiments were conducted at an ambient temperature of 25ºC.

3. Results and discussion

3.1. Permeation data

The mass transport coefficients of analysed gases for chosen magnetic hybrid membranes with magnetic micropowders MQP-16-7, MQP-B and MQP-14-12 were collected in Tab. 1 and 2. Data calculated on the basis of eq. 1-6, are the mean values of six measurements with standard deviations not greater than 15%.

3.2. Magnetic properties

The example of demagnetization curves (II quarter of a hysteresis loop) of the magnetic hybrid membranes with various types of added magnetic fillers are shown in Fig.1.

The shape of the hysteresis loops and the course of magnetization evidenced the hard magnetic character of tested materials.

TABLE 1

Mass transport coefficients of pure oxygen and nitrogen for various magnetic hybrid membranes

Membrane	$\alpha_{O2/N2}$	N_2 pure				O_2 pure			
		$\bar{D}$	D_L	P	S	$\bar{D}$	D_L	P	S
		$\cdot 10^7$ (cm^2/s)		(Barrer)	$\cdot 10^3$(cm^3STP/ cm^3cmHg)	$\cdot 10^7$ (cm^2/s)		(Barrer)	$\cdot 10^3$(cm^3STP/ cm^3cmHg)
EC	1.45	3.70	3.70	0.80	0.22	11.00	10.00	1.16	0.11
EC, 1.5g, MQFP-14-12, 25 μm	2.44	17.52	13.22	42.82	2.42	48.31	64.91	101.80	2.11
EC, 1.5g, MQP-14-12, 20-50 μm	1.99	14.51	11.81	34.93	2.40	35.20	47.65	72.69	2.07
PPO	3.80	0.80	0.70	3.80	4.75	1.70	1.80	14.40	8.47
PPO, 1.0g, MQFP-16, 5 μm	4.41	2.97	2.92	16.18	5.45	6.21	8.14	71.41	11.51
PPO, 1.75g, MQFP-16, 5 μm	4.90	4.94	4.72	37.84	7.66	15.41	20.30	185.30	12.03
PPO, 1.1g, MQFP-B, 5 μm	4.50	3.14	3.08	18.07	5.75	7.01	9.20	81.36	11.61
PPO, 1.5g, MQFP-B, 5 μm	4.77	4.03	3.89	27.81	6.90	11.15	14.67	132.57	11.89

TABLE 2

Mass transport coefficients of oxygen and nitrogen in air for various magnetic hybrid membranes

Membrane	$\alpha_{O2/N2}$	N_2 in air				O_2 in air			
		$\bar{D}$	D_L	P	S	$\bar{D}$	D_L	P	S
		$\cdot 10^7$ (cm^2/s)		(Barrer)	$\cdot 10^3$(cm^3_{STP}/ cm^3cmHg)	$\cdot 10^7$ (cm^2/s)		(Barrer)	$\cdot 10^3$(cm^3_{STP}/ cm^3cmHg)
EC	1.53	9.00	9.00	15.00	2.00	15.00	15.00	23.00	1.52
EC, 1.5g, MQFP-14-12, 25 μm	2.56	76.13	81.38	140.07	1.87	143.50	162.17	358.80	2.50
EC, 1.5g, MQP-14-12, 20-50 μm	2.34	56.73	61.58	103.52	1.80	99.97	113.83	242.23	2.33
PPO	3.04	0.80	0.80	4.82	6.02	1.80	1.90	14.65	8.14
PPO, 1.0g, MQFP-16, 5 μm	3.85	5.07	4.08	27.40	5.40	12.51	9.80	105.43	8.43
PPO, 1.75g, MQFP-16, 5 μm	4.36	10.81	8.66	64.73	5.99	31.13	25.77	281.96	9.06
PPO, 1.1g, MQFP-B, 5 μm	3.94	5.57	4.48	30.66	5.50	14.14	11.19	120.86	8.55
PPO, 1.5g, MQFP-B, 5 μm	4.22	8.15	6.54	47.45	5.82	22.51	18.37	200.24	8.90

TABLE 3

Magnetic properties of organic-inorganic hybrid membranes

Membrane	Coercivity [kA/m]	Remanence [emu/g]	Saturation magnetization [emu/g]	w [cm/s]
EC, 1.5g, MQFP-14-12, 25 μm	950	35.43	50.07	$6{,}59.10^{-4}$
EC, 1.5g, MQP-14-12, 20-50 μm	911	34.84	49.87	$3{,}68.10^{-4}$
PPO, 1.0g, MQFP-16, 5 μm	555	29.09	51.45	$8{,}72.10^{-5}$
PPO, 1.75g, MQFP-16, 5 μm	568	44.83	75.54	$1{,}34.10^{-4}$
PPO, 1.1g, MQFP-B, 5 μm	744	47.69	70.46	$9{,}93.10^{-5}$
PPO, 1.5g, MQFP-B, 5 μm	730	48.49	74.43	$1{,}20.10^{-4}$

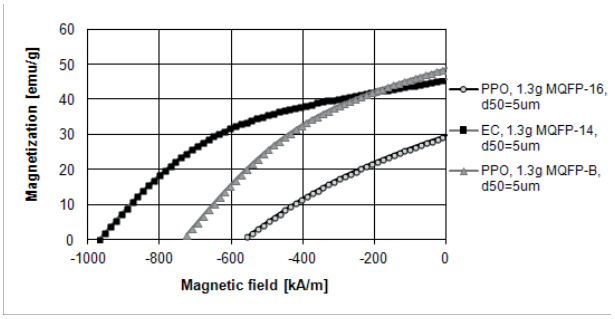

Fig. 1. Demagnetization curves (II quarter of a hysteresis loop) of magnetic hybrid membranes with different magnetic powders

The coercivity, remanence, saturation magnetization and oxygen drift coefficient values for obtained hybrid membranes were given in Table 3.

The results given in Figure 1, Table 3 and from earlier studies [21, 22, 27, 30, 37] showed that the remanence and saturation magnetization increased with the increase of the powder addition in the membrane. It was found that the character of this dependency for saturation magnetization is linear. The third parameter, coercivity depended on a composition and microstructure of the magnetic powder but not on its participation in the polymer matrix. Furthermore, the type of added magnetic powders had an influence on

membrane's magnetic properties. Namely, partial substitution of neodymium by praseodymium results in an improvement of MQP-16-7 (alloy Nd-Pr-Fe-B) magnetic properties, like the magnetization. This significant change was caused by the formation of iron dendrites and greater magnetocrystalline anisotropy of $Pr_2Fe_{14}B$ phase. In the case of MQP-14-12 (alloy Nd-Nb-Fe-B) niobium addition creates precipitates of type Nb_2FeB and nanoscale precipitates, inside the $Nd_2Fe_{14}B$ phase grains, which in turn anchor the domain walls and lead to a significant increase in coercivity. While the partial substitution of iron by cobalt results in the increase of Curie temperature and the coercivity in MQFP-B (alloy Nd-Fe-Co-B) [20].

Additionally, the coercivity, remanence and saturation magnetization values for membranes with powders of grain size 5 and 25 μm may be influenced by the fact that these powders are coated with an inorganic coating AA4. It was stated that magnetic properties of the magnetic hybrid membranes depend mainly on the type, particle size and addition of the magnetic powder, and to a minor degree on the type of polymer matrix. That means that the magnetic properties of these membranes, and their potential usage in the future could be appropriately tuned and tailored. This will have a direct impact on the gas separation and transport properties of these membranes.

The results presented in Tables 1-3 prove that values of remanence and the gas transport coefficients (*D*, *P*, *S* and *α*) are growing with the decrease of magnetic powder particle size and rise of its addition. However, the greatest coefficient's value increase is observed for the paramagnetic oxygen. The coercivity depends mainly on the remanence, that largely affects the properties of the concerned hybrid membranes. So, the effect of coercivity on the transport and separation properties of the membrane is indirect. The values of saturation magnetization, separation and gas transport coefficients of hybrid membranes are growing (Fig. 2) with the increase of the magnetic powder amount. It was also observed that the influence of remanence on the separation (coefficient *α*) and transport properties of membranes (coefficient's *P*, *D*, *S*) is much greater than this of saturation magnetization. The small increase of a nitrogen diffusion coefficient with the rise of the saturation magnetization value, could be associated with the changes in the membrane microstructure.

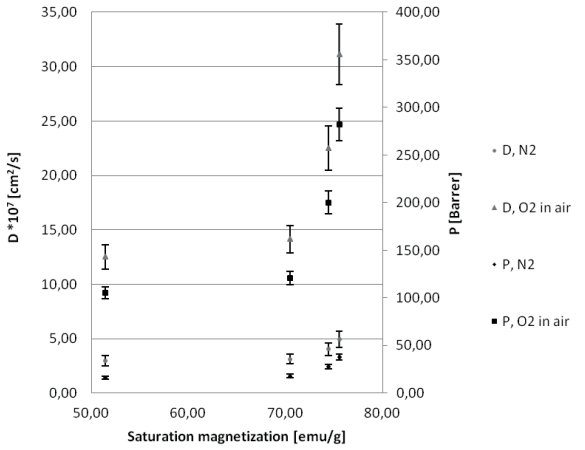

Fig. 2. Dependence of diffusion and permeation coefficients on PPO magnetic hybrid membrane's saturation magnetization

Based on the data given in Table 3 it was found that the remanence and saturation magnetization increase and coercivity decrease, caused the rise of a drift coefficient *w*, particularly in the case of a paramagnetic oxygen.

3.3. Results of mechanical measurements

Potential future use of magnetic hybrid membranes in gas mixture separation requires having the appropriate mechanical properties and strength. That's why the mechanical and rheological measurements for these membranes were performed. The following mechanical parameters: apparent yield strength $\mathbf{R_{0,2}}$, real yield strength **R**, tensile strength $\mathbf{R_m}$ and Young's modulus **E** were determined for the tested samples.

A study of mechanical properties showed that the increase of the magnetic powder addition (from 1.1 to 1.5g) and a decrease of its granulation (from 25 to 5 μm) improved mechanical properties of the tested membranes such as: apparent yield strength, real yield strength (increase from 7.39 to 10.66 MPa), tensile strength (rise from 12.58 to 18.54 MPa) and Young's modulus (growth from 289.1 to 705.7 MPa). Much better mechanical properties were stated for hybrid membranes with PPO matrix, that is resulted from PPO better mechanical properties in comparison with EC [38, 39]. The improvement of hybrid membrane's mechanical properties is probably connected with the reduction of overall polymer chain's mobility and increase of density of hybrid membranes with the addition of magnetic micropowders. That was confirmed by X-ray micro-tomography examinations, in which the more compacted structure of the hybrid membranes was revealed.

Enhancement of the mechanical properties translates directly into better separation properties of hybrid membranes and their potential use in the future.

Because the images taken by optical microscopy (Fig.3.) did not allow for more detailed examination of the magnetic membrane's structure, it was decided to apply the technique of X-ray micro-tomography. The example results from the X-ray micro-tomography for PPO hybrid membrane with 1.75g of MQFP-16-7 are shown in Fig.4.

In the Figure 4 are shown the results concerning orientation of the areas occupied by the magnetic particles. The black colour indicates the magnetic particles, and the grey is a polymer matrix. The direction of the longest line that can be routed through a single area occupied by the particles was measured. It was found that the maximum is approximately 90 degrees. This fully confirms previous observations concerning the perpendicular orientation of created magnetic particle's chains (linked with magnetic forces within the polymer matrix) which form the magnetic channel structure.

The concept of magnetic channels, formed by the magnetic powder particles in the polymer matrix under the influence of the applied magnetic field was introduced in the earlier works. It was also discussed the role of these channels in the separation of oxygen and nitrogen, characterized by various magnetic properties and in a different way interacting with those magnetic channels [30, 32-34].

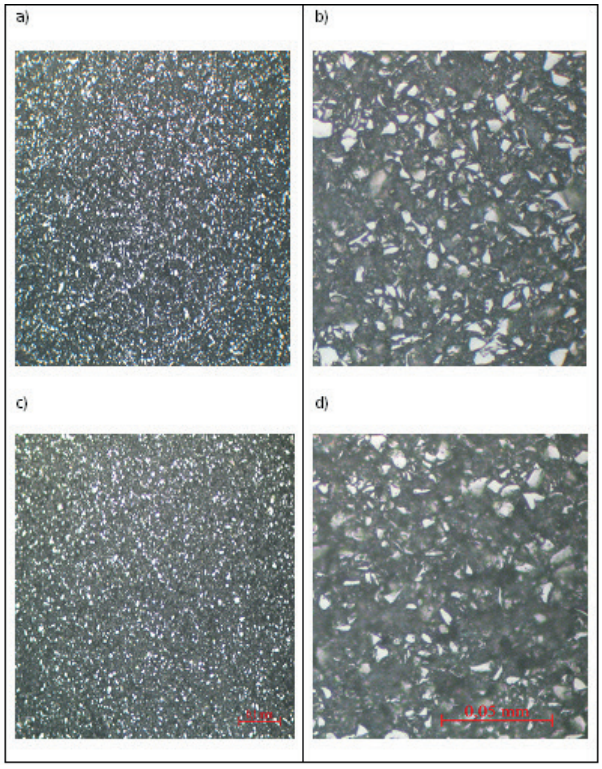

Fig. 3. Optical microscope images of the PPO magnetic membrane with various additions of MQP-16-7, 5 μm: a) 1.00g (magnification 20x), b) 1.00g (magnification 50x), c) 1.75g (magnification 20x) d) 1.75g (magnification 50x)

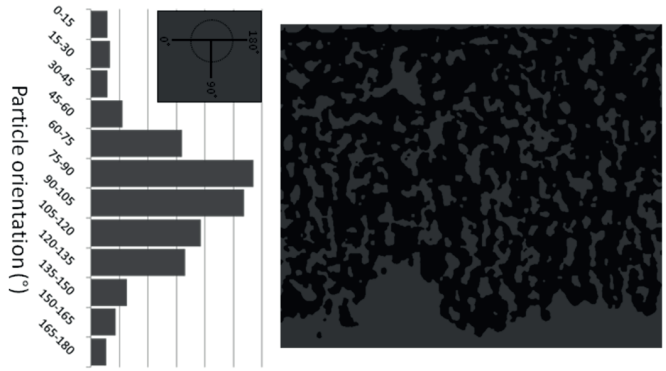

Fig. 4. X-ray micro-tomography visualization of the area's orientation occupied by the magnetic powder particles within the magnetic hybrid membrane structure

3.4. Results of rheological analysis

The obtained magnetic hybrid membranes combine the features of the elastic solid and the viscous liquid. Such materials, could be characterized by means of viscoelastic properties. To describe the rheological properties of such materials, there are three parameters, such as: the storage modulus, *G'*, the loss modulus, *G"* and the loss coefficient tan *δ* [40, 41].

In this study, the elastic (storage) modulus *G'* and the loss modulus, *G"* were measured as a function of an angular frequency ω and strain [%]. The example rheological results for 3 chosen membranes were shown in Fig.5.

The storage modulus G' increases significantly with the increase of the magnetic powder addition (Fig.5). It was stated that for the examined hybrid membranes, the value of loss modulus G" is lower by one order of magnitude than the storage modulus G', while the values of tan δ vary to a small extent. The values of G' modulus for the EC hybrid membrane are one order smaller than for the PPO hybrid membranes. It is probably connected with various types of membrane matrices, characterized by different rheological properties. The intersection of function G' and G" indicates the crossover point. At this point, the samples become more viscous than elastic. In the case of EC magnetic hybrid membrane, the point of intersection was about 1% strain, while in the case of PPO hybrid membranes in about 3%. So, for the PPO hybrid membranes this change occurs for higher strain values. It was stated that the best resistance to elastic deformation has the hybrid PPO membrane with 1.75 g of dispersed magnetic powder, while the most resistant to viscous flow was membrane with 1.0 g of magnetic powder. Significant higher values of G' for membrane with the highest magnetic powder content are due to the higher amount of ferromagnetic particles in the polymer matrix (the stiffness of magnetic particles is incomparable higher than the stiffness of the polymer matrix). Moreover, with the increase of magnetic powder addition, the distance between magnetic particle chains decreases, the magnetic interaction between them rises, what leads to formation of more complex microstructures similar to the 3D matrices with higher storage modules. Lower values of rheological parameters were noted for membrane containing powder with larger granulation, wider distribution of magnetic particle size and thereby much lower degree of space filling by magnetic powder.

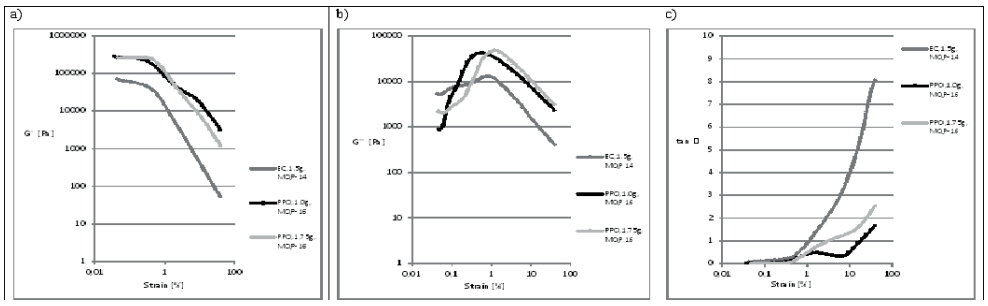

Fig. 5. Comparison of the dependency of a) storage modulus G', b) loss modulus G" and c) loss coefficient tan δ versus strain [%] for three various magnetic hybrid membranes

4. Conclusions

Magnetic hybrid organic-inorganic membranes were successfully synthesized on the basis of ethylcellulose and poly(2,6-dimethyl-1,4-phenylene oxide) polymer matrices and various magnetic powder microparticles. It was stated that the separation and gas transport properties of the magnetic hybrid membranes were enhanced with the increase of magnetic powder addition, accompanied by an increase in membrane's remanence and saturation magnetization. Whereby the influence of remanence on the separation (coefficient α) and transport properties of membranes (coefficient's P, D, S) is much greater than this of saturation magnetization. At the same time, it was observed that the decrease in powder particle size, accompanied by an increase of the membrane's coercivity and remanence also positively influenced the gas transport and separation properties (higher gas permselectivity, permeability and to a lesser degree solubility) of investigated magnetic hybrid membranes. It was also found that the increase of the remanence and saturation magnetization causes an increase of a drift coefficient w, particularly in the case of a paramagnetic oxygen. It can be assumed, that the magnetic properties of the magnetic hybrid organic-inorganic membranes depend mainly on the type, the particle size and addition of the magnetic micropowder, and to a minor degree on the type of polymer matrix. That means that the total magnetic behaviour of these magnetic hybrid membranes could be tuned and tailored depending on these parameters.

In turn, the increase of the magnetic powder addition, decrease of its granulation and selection of appropriate type of polymer matrix improved mechanical (increase of apparent yield strength $\mathbf{R}_{0,2}$, real yield strength $\mathbf{R}$, tensile strength $\mathbf{R}_m$ and Young's modulus $\mathbf{E}$) and rheological parameters of the tested membranes. It was stated that the hybrid membrane's resistance to elastic deformation increased with the rise of magnetic powder addition, while their resistance to viscous flow decreases. The improvement of their mechanical and rheological properties also had a positive effect on their gas separation properties. Proper selection of all discussed parameters will have a direct impact on the separation and transport properties of investigated membranes and will affect their potential application in the future.

Acknowledgements

The authors would like to thank Professor Z. J. Grzywna for substantive support, Dr. Stefan Awietjan and Dr. Jakub Jaroszewicz for their assistance with the X-ray micro-tomography and rheological analysis.

REFERENCES

[1] F. Li, Y. Li, T.-S. Chung, S. Kawi, J. Membr. Sci. **356**, 14 (2010).

[2] B. Freeman, Y. Yampolskii, I. Pinnau, Materials Science of Membranes for Gas and Vapor Separation, John Wiley and Sons, 2006.

[3] M. Aparicio, A. Duran, J. Sol-Gel Sci. Technol. **31**, 103 (2004).

[4] G. Defontaine, A. Barichard, S. Letaief, C. Feng, T. Matsuura, C. Detellier, J. Colloid Interface Sci. **343**, 622 (2010).

[5] Z. He, I. Pinnau, A. Morisato, Desalination **146**, 11 (2002).

[6] C. Hibshman, C.J. Cornelius, E. Marand, J. Membr. Sci. **211**, 25 (2003).

[7] S. M. Kumbar, T. Selvam, C. Gellermann,W. Storch, T. Ballweg, J. Breu, G. Sextl, J. Membr. Sci. **347**, 132 (2010).

[8] H. Rao, Z. Zhang, C. Song, T. Qiao, S. Xu, Sep. Purif. Technol. **78**, 132 (2011).

[9] D.Q. Vu, W.J. Koros, S.J. Miller, J. Membr. Sci., **211**, 311 (2003).

[10] R.M. Dukali, I. Radovic, D.B. Stojanovic, P.S. Uskokovic, N. Romcevic, V. Radojevic, R. Aleksic, J. Alloys Compd. **583**, 376 (2014).

[11] K.G. Chandrappa, T.V. Venkatesha, J. Alloys Compd. **542**, 68 (2012).

[12] J. Hradil, P. Sysel, L. Brožová, J. Kovářová, J. Kotek, React. Funct. Polym. **67**, 432 (2007).

[13] E. Minko, P. Sysel, M. Hauf, J. Brus, L. Kobera, Macromol. Symp. **295**, 88 (2010).

[14] D. Sieffert, C. Staudt, Sep. Purif. Technol. **77**, 99 (2011).

[15] P. Sysel, E. Minko, M. Hauf, K. Friess, V. Hynek, O. Vopicka, K. Pilnacek, M. Sipek, Desalin. Water Treat. **34**, 211 (2011).

[16] H. Maachou, K. Bal, Y. Bal, A. Chagnes, G. Cote, D. Aliouche, Appl. Biochem. Biotechnol. **168**, 1459 (2012).

[17] B. Belaabed, J.L. Wojkiewicz, S. Lamouri, N. El Kamchi, T. Lasri, J. Alloys Compd. **527**, 137 (2012).

[18] R.M. Khafagy, J. Alloys Compd. **509**, 9849 (2011).

[19] L. Zheng, W. Li, M. Zhu, L. Ye, W. Bi, J. Alloys Compd. **560**, 80 (2013).

[20] M. Leonowicz, J.J. Wysłocki, Współczesne magnesy. Technologie, mechanizny koercji, zastosowania. WNT, Warszawa 2005.

[21] M. Bystrzejewski, O. Łabedź, W. Kaszuwara, A. Huczko, H. Lange, Powder Technol. **246**, 70 (2013).

[22] I. Gancarz, J. Bryjak, M. Bryjak, W. Tylus, G. Poźniak, Eur. Polym. J. **4**, 2430 (2006).

[23] G. Dudek, R. Turczyn, A. Strzelewicz, M. Krasowska, A. Rybak, Z.J. Grzywna, Sep. Purif. Technol. **109**, 55 (2013).

[24] M.A. Ahmed, R.M. Khafagy, S.T. Bishay, N.M. Saleh, J. Alloys Compd. **578**, 121 (2013).

[25] A. Rybak, Z. J. Grzywna, W. Kaszuwara, J. Membr. Sci. **336**, 79 (2009).

[26] A. Rybak, A. Strzelewicz, M. Krasowska, G. Dudek, Z.J. Grzywna, Sep. Sci. Technol. **47**, 1395 (2012).

[27] A. Rybak, M. Krasowska, A. Strzelewicz, Z. J. Grzywna, Acta Phys. Pol. B **40**, 1447 (2009).

[28] Z.J. Grzywna, A. Rybak, A. Strzelewicz, Air enrichment by polymeric magnetic membranes, chapter 9 in a book: Membrane Gas Separation, ed. B. Freeman, Y. Yampolskii, John Wiley & Sons, (2010).

[29] M. Krasowska, A. Rybak, K. Pawełek, G. Dudek, A. Strzelewicz, Z.J. Grzywna, J. Membr. Sci. **415-416**, 864 (2012).

[30] Z.J. Grzywna, A. Rybak, P. Borys, K. Pawełek, J. App. Membr. Sci. Tech. **14**, 31-40 (2011).

[31] A. Rybak, Z.J. Grzywna, P. Sysel, Sep. Purif. Technol. **118**, 424 (2013).

[32] A. Rybak, G. Dudek, M. Krasowska, A. Strzelewicz, Z.J. Grzywna, P. Sysel, Chem. Pap. **68** (10), 1332 (2014).

[33] A. Rybak, G. Dudek, M. Krasowska, A. Strzelewicz, Z.J. Grzywna, Sep. Sci. Technol., **49**, 1729 (2014).
[34] P. Borys, A. Rybak, Z.J. Grzywna, Ind. Eng. Chem. Res. **52**, 8887 (2013).
[35] A. Strzelewicz, M. Krasowska, G. Dudek, A. Rybak, M. Cieśla, Acta Phys. Pol., B **44**, 955 (2013).
[36] A. Rybak, W. Kaszuwara, J. Alloys Compd., 2015 – in press.
[37] S. Kangarlou, I. Haririan, Iran. J. Pharm. Sci. **3**, 135 (2007).
[38] C. P. Tsui, C. Y. Tang, T. C. Lee, Polym. Compos. **22**, 6 (2001).
[39] A. Boczkowska, S.F. Awietjan, S. Petrzko, K.J. Kurzydłowski, Composites B **43**, 636 (2012).
[40] A. Boczkowska, S.F. Awietjan, J. Mater. Sci. **44**, 4104 (2009).